ISSN (Print) 1226-1750
ISSN (Online) 2233-6656
Journal of Magnetics 28(4), 488-492 (2023) https://doi.org/10.4283/JMAG.2023.28.4.488

A Study on Increasing the Useful Field of View of Gamma Camera through the Expansion of the Use of Photosensors

Seung-Jae Lee[1,2], Byungdu Jo[1,2], and Cheol-Ha Baek[3]*

[1]*Department of Radiological Science, Dongseo University, Busan 47011, Republic of Korea*
[2]*Center for Radiological Environment & Health Science, Dongseo University, Busan 47011, Republic of Korea*
[3]*Department of Radiological Science, Kangwon National University, Samcheok 25949, Republic of Korea*

(Received 17 October 2023, Received in final form 11 December 2023, Accepted 11 December 2023)

A new gamma camera was designed to reduce edge effect that can occur in conventional gamma cameras and increase the useful field of view (UFOV). In order to reduce edge effect and increase UFOV, a new gamma camera was designed to collect light incident on the side of the scintillator by plaing an additional photosensor used in the conventional gamma camera to prevent the occurrence of edge effect. DETECT2000 was used to evaluate the useful field of view of the desinged gamma camera and the conventional gamma camera. As a result, the UFOV of the new gamma camera was improved by about 95.8 % compared to the UFOV of the conventional gamma camera. If the results of this study are used when designing a gamma camera, it is considered that edge effects can be prevented and an expanded UFOV can be achieved.

Keywords : gamma camera, edge effect, useful field of view, magnetic field, electromagnetic radiation

1. Introduction

Nuclear medicine imaging devices are used to diagnose various diseases that can occur in the human body early and to observe subtle changes in lesions [1]. Representative biological imaging technologies include a gamma camera and a single photon emission tomography device that acquires tomographic images by rotating the gamma camera [2, 3]. A gamma camera is a device that detects and images gamma rays generated from radioactive isotopes injected into the human body. It plays a significant role in improving the quality of life by using it for early diagnosis of diseases. In the detection process of this gamma camera, the light generated by the interaction between the gamma ray and the scintillator diffuses within the scintillator, and the light is collected by a photosensor coupled to the scintilator, and then the location where the gamma ray and the scintillator interacted is imaged based on the size of the signal. However, in these gamma cameras, light gathers at the edge of the scintillator, creating an edge effect that reduces uniformity, reducing the useful field of view (UFOV) and deteriorating uniformity [4].

In this study, we designed a gamma camera that reduces the occurrence of such edge effects and increases the UFOV. An increase in the UFOV increases the range that can be examined in a single examination, which can reduce the total examination time and thereby reduce the patient's radiation dose. Additionally, cost reduction can be achieved by relatively reducing the size of the scintillator, which costs the most when manufacturing a gamma camera. In order to increase the UFOV and evaluate the performance of the designed gamma camera, we designed and evaluated the gamma camera using DETECT2000 [5, 6], which can simulate the light generated within the detector.

2. Materials and Methods

2.1. Design gamma camera

In order to increase the UFOV by reducing the edge effect generated by the gamma camera, a gamma camera used previously and an edge effect reduction gamma camera were designed. Fig. 1 shows the configuration of a conventional gamma camera. A gamma camera consisting of a scintillator and a photosensor generates light by interacting with gamma rays from the scintillator, and this light is collected by a photosensor to calculate the

*Corresponding author: Tel: +82-33-540-3384
Fax: +82-33-540-3389, e-mail: baekch100@gmail.com

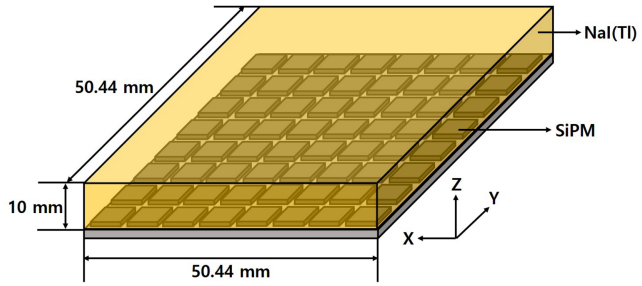

Fig. 1. (Color online) A conventional gamma camera where the photosensor is located below the scintillator.

location where the gamma ray and the scintillator interacted. In the conventional gamma camera, NaI(Tl) was used as the scintillator, and considering the size of the photosensor used, the scintillator size was designed to be 50.44 mm × 50.44 mm × 10 mm. The photosensor used a silicon photomultiplier (SiPM). It consists of 8 × 8 arrays of SiPM pixels active area 6 mm × 6 mm, resulting in a total size of 50.44 mm × 50.44 mm [7, 8]. SiPM is a semiconductor optical sensor that is very small in size compared to photomultiplier tubes and is used in various nuclear medicine devices. Additionally, it is not affected by magnetic field, so it can be used in detectors that operate within magnetic fields. The newly designed gamma camera to increase the UFOV by reducing edge effects is shown in Fig. 2. An additional photosensor was placed on the side of the conventional gamma camera's scintillator to prevent light from gathering at the edges and measure light signals. The size of the scintillator of the gamma camera that increases the UFOV is the same as that of the conventional gamma camera, and the photosensor also uses the same SiPM. The photosensor used on the side was a SiPM with a size of 6 mm × 6 mm, and 8 SiPMs were used on each side.

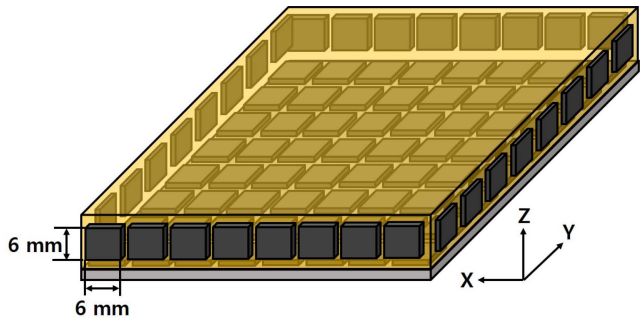

Fig. 2. (Color online) A gamma camera designed to improve the useful field of view by placing an additional photosensor on the side of the scintillator to the conventional gamma camera.

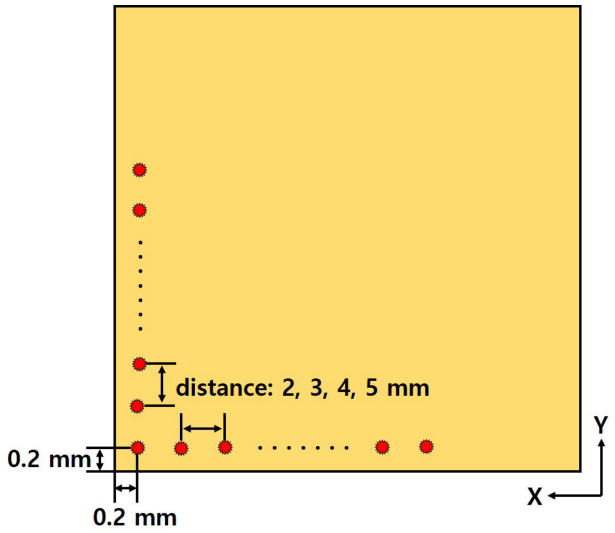

Fig. 3. (Color online) Gamma-ray events are generated at intervals of 2, 3, 4 and 5 mm from a point 0.2 mm away from the corner of the scintillator on the X and Y axes.

2.2. Gamma-ray event generating and flood image acquisition

In order to evaluate the degree of increase in the UFOV of the newly designed gamma camera, we simulated a series of processes in which gamma rays and scintillator interact to generate light, and this generated light is measured by a photosensor and obtained as a position signal. The locations where gamma rays and scintillator interacted were designated, and the number of lights generated by 140 keV gamma rays interacting with NaI(Tl) scintillator at each designated location was calculated based on the number of lights and the efficiency obtained from SiPM. The location of the gamma-ray interaction occurs in all scintillator areas at the center of the scintillator height at 2 mm, 3 mm, 4 mm, and 5 mm intervals at points 0.2 mm apart in the X and Y axes from the corner point, as shown in Fig. 3. The maximum detectable area was analyzed.

3. Results

3.1. Flood images acquired according to gamma-ray event intervals

Flood images of the location where the scintillator and gamma rays interacted were obtained from the conventional gamma camera and the newly designed gamma camera. As shown in Fig. 4, the interacting positions were reconstructed into images according to the gamma-ray event occurrence interval, and overlap occurred according to the gamma-ray event occurrence interval. In conven-

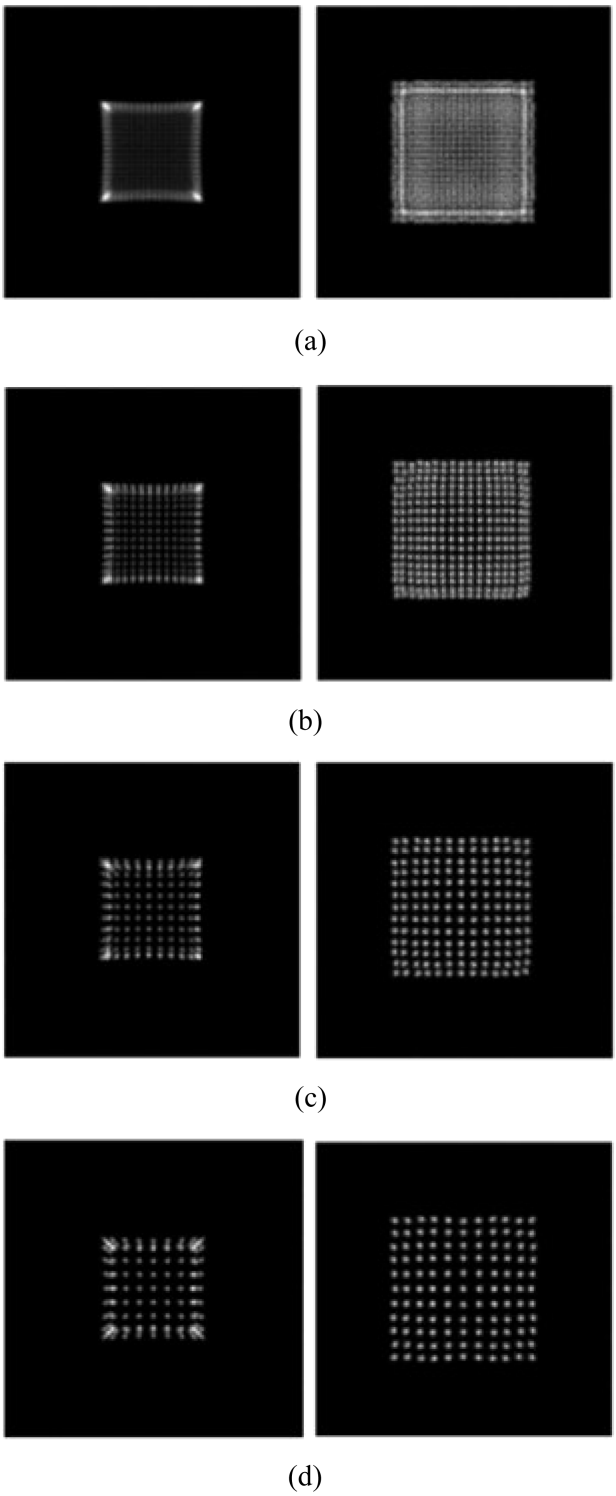

Fig. 4. Flood images acquired at each gamma-ray event interval. (a) 2 mm, (b) 3 mm, (c) 4 mm, (d) 5 mm interval. At each interval, left: conventional gamma camera, right: new gamma camera.

tional gamma camera, edge overlap occurred at all intervals. In particular, the corners appeared bright in the image as overlap occurred at all intervals along the X and Y axes. However, in the newly desinged gamma camera, when gamma ray events were generated at intervals of 2 mm, overlap occurred, but at the remaining intervals, all locations appeared as images separated without overlap.

3.2. Profile of flood imgae

To evaluate the degree of overlap near the edge of the flood image, the profile of the flood image was obtained. Fig. 5 shows the profile of the flood image according to the occurrence interval of each gamma-ray event obtained from the conventional gamma camera and the newly designed gamma camera. In conventional gamma cameras, overlap occurred at all intervals. At 2 mm intervals, six points of overlap occurred near the edge, at 3 mm intervals, four points overlapped, at 4 mm intervals, three points overlapped, and at 5 mm intervals, overlaps occurred at three points. Accordingly, the maximum area where the scintillator can be used was calculated to be approximately 30.0 mm × 30.0 mm. In the newly designed gamma camera, overlap occurred at three points at 2 mm, and all remaining intervals appeared separated in the image. In Fig. 6, the edge overlap in the profiles of the conventional gamma camera and the newly designed gamma camera acquired at 2 mm intervals is shown. Accordingly, the UFOV of the newly desinged gamma camera was calculated to be approximately 42.0 mm × 42.0 mm.

4. Discussion and Conclusion

The light generated by the interaction of the scintillator and gamma rays moves within the scintillator, and is detected by the photosensor at the edge through the reflector on the side of the scintillator, causing an overlap phenomenon at the edge. To solve this problem, we designed a gamma camera that places a photosensor on the side of the scintillator in addition to the photosensor arrangement used in the conventional gamma camera. Through this, it was confirmed that the UFOV was increased compared to the conventional gamma camera by reducing the edge effect that reduces the UFOV of the gamma camera. Gamma-ray events were generated within the scintillator at intervals ranging from 2 mm to 5 mm, and light was collected through a photosensor, which was reconstructed into a flood image. In the conventional gamma camera, overlap occurred at the edges at all intervals, but in the newly designed gamma camera, overlap occurred only at 2 mm and appeared separated at all remaining intervlas. In the conventional gamma camera, the 2 mm interval image overlapped from the

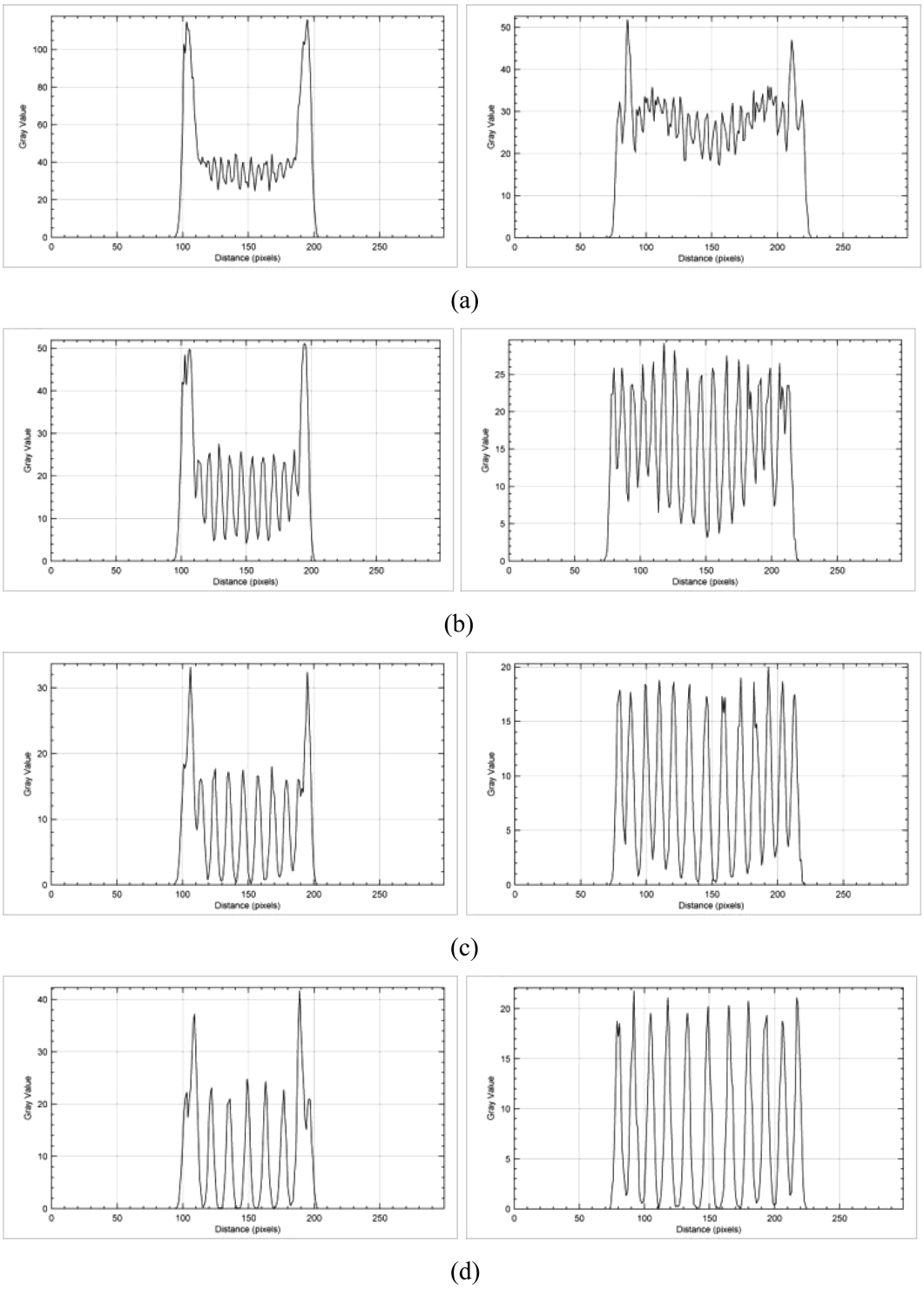

Fig. 5. Profile of flood images according to the interval of occurrence of each gamma-ray event obtained from the conventional gamma camera and the new gamma camera. (a) 2 mm, (b) 3 mm, (c) 4 mm, (d) 5 mm interval. At each interval, left: conventional gamma camera, right: new gamma camera.

edge to the location of the sixth gamma-ray event, but in the newly designed gamma camera, the overlap appeared only up to the location of the third gamma-ray event. As a result of calculating the UFOV through this, as shown in Fig. 7, the conventional gamma camera has an UFOV of about 35.5 % of the total scintillator area, while the newly

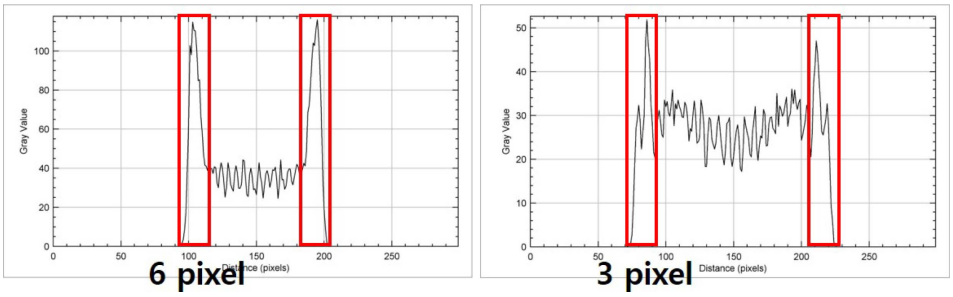

Fig. 6. (Color online) Overlapping at the edges occurred in the profiles of the conventional and new gamma cameras acquired from gamma-ray events spaced 2 mm apart. Left: conventional gamma camera result, Right: new gamma camera result.

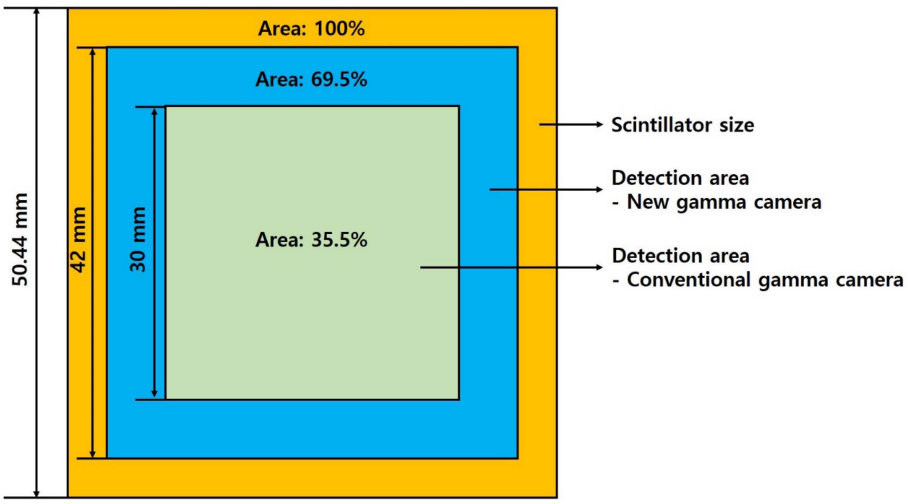

Fig. 7. (Color online) Comparison results of the useful field of view between the conventional gamma camera and the new gamma camera.

designed gamma camera has an UFOV of about 69.5 %, compared to the conventional gamma camera. Compared to this, the detectable area was improved by about 95.8 %.

When using the gamma camera designed in this study, the UFOV can be improved, allowing a larger area to be acquired in a single examination when examining a patien. Accordingly, it is considered that the amount of radiation dose can be reduced by reducing the examination time and the amount of radioisotope injected into the patient.

Acknowledgments

This work was supported by Dongseo University, “Dongseo Cluster Project” Research Fund of 2023 (DSU-20230003).

References

[1] Y. S. Han, S. W. Park, S. Y. Seo, C. S. Park, and M.-S. Han, J. Korean Magn. Soc. **31**, 1 (2021).
[2] V. Ilisie, L. Moliner, S. Oliver, F. Sanchez, A. J. Gonzalez, M. Seimetz, M. J. Rodriguez-Alvarez, abd J. M. Benlloch, Sci. Rep. **9**, 18431 (2019).
[3] R. J. Jaszczak, R. E. Coleman, and C. B. Lim, IEEE Trans. Nucl. Sci. **27**, 1137 (1980).
[4] J. Y. Hwang, S.-J. Lee, C.-H. Baek, K. H. Kim, and Y. H. Chung, Nucl. Instrum. Methods Phys. Res. A **633**, S166 (2011).
[5] F. Cayouette, C. Moisan, N. Zhang, and C. J. Thompson, IEEE Trans. Nucl. Sci. **49**, 624 (2002).
[6] F. Cayouette, D. Laurendeau, and C. Moisan, Proceedings of SPIE **4833**, 69 (2003).
[7] T. Huang and Z. Zhang, Nucl. Instrum. Methods Phys. Res. A **999**, 165225 (2021).
[8] https://www.onsemi.com/download/data-sheet/pdf/arrayj-series-d.pdf